Dipole interactions in electrofusion

Contributions of membrane potential and effective dipole interaction pressures

David A. Stenger,* Karan V. I. S. Kaler,‡ and Sek Wen Hui*

*Membrane Biophysics Laboratory, Roswell Park Cancer Institute, Buffalo, New York 14263 USA; and ‡Department of Electrical Engineering, University of Calgary, Calgary, Canada T2N 1N4

ABSTRACT The contributions of pulse-induced dipole–dipole interaction to the total pressure acting normal to the membranes of closely positioned pronase treated human erythrocytes during electrofusion was calculated. The total pressure was modeled as the sum of pressures arising from membrane potential and dipole–dipole attraction opposed by interbilayer repulsion. The dipole–dipole interaction was derived from the experimentally obtained cell polarizability. The threshold electric field amplitude necessary for fusion of pronase-treated human erythrocytes was experimentally obtained at various combinations of pulse duration, frequency, and the conductivity of the external medium. The theoretical values of the critical electric field amplitude compared favorably to the experimentally obtained threshold field amplitudes. Fusion by dc pulses may be primarily attributed to attainment of sufficiently high membrane potentials. However, with decreasing external conductivity and increasing sinusoidal pulse frequency (100 kHz–2.5 MHz), the induced dipole–dipole interactions provide the principal driving force for membrane failure leading to fusion.

INTRODUCTION

Since the time of the earliest observations of electrofusion, the reversible dielectric breakdown of the membranes has been viewed as the most critical event affecting the process. Recent work by Needham and Hochmuth (1989) on the electric breakdown of liposomes has demonstrated quantitatively that membrane failure is indeed a combined result of the lateral isotropic tension and the normal pressure caused by the membrane potential. However, when applied to electrofusion between cells, the membrane potential theory is no longer sufficient because pronase treated red blood cells (PRBC) could be induced to fuse with high frequency (1–3 MHz) ac pulse amplitudes and durations comparable to those of dc pulses (see Results). The membrane potential predicted for ac fields (Holzapfel et al., 1982; Zimmermann, 1986) state that the membrane potential is inversely proportional to $\omega\tau_m$, where ω is the angular frequency of the sinusoidal field and τ_m is the membrane charging relaxation time. This implies a decrease in the membrane potential of several orders of magnitude for a given field amplitude as the frequency is increased from dc to several megahertz. A similar inconsistency was noted by Chang (1989) using dc offset sinusoidal pulses on intact red blood cells (RBC) in higher conductivity media.

A factor which is often overlooked in the theory of electrofusion is the pressure exerted by the pulse-induced dipoles on the contacting membrane pair between cells in a pearl chain. Cell alignment before high field pulse application is attributed to the mutual attraction of electrically induced dipoles. However, the magnitude of such forces, and the role of dipole–dipole interactions in the mutual approach and direct contact of membranes caused by the high electric field pulse(s) have not been formally considered. This is due in large part to the lack of complete frequency domain data concerning the effective polarizability of cells relative to their suspending media.

In general, biological cells exhibit two distinct, principal mechanisms for development of an effective dipole moment when suspended in media having conductivities in the range of 10–1,000 μS/cm. The first of these, the counter ion polarization, occurs at low frequencies ($<10^4$ Hz). It has been attributed to the field-induced redistribution of counter ions in the electrical double layer of the exterior membrane surface (Pohl, 1978; Sauer and Schlogl, 1985). However, at frequencies $> 10^4$ Hz, the above polarization gives way to a Maxwell-Wagner type of interfacial polarization (Pohl, 1978). The minimum frequency for which this type of polarization occurs is dependent on the conductivity of the cell interior σ_i, relative to that of the suspending medium, σ_e. This minimum frequency shifts to progressively higher frequencies as the conductivity of the suspending medium is increased.

The recently developed method of active feedback-

Dr. David A. Stenger's present address is Center for Bio/Molecular Science and Engineering, Code 6090, Naval Research Laboratory, Washington, DC 20375.

0006-3495/91/05/1074/11 $2.00

controlled DEP levitation (Jones and Kraybill, 1986; Kaler and Tai, 1988; Kaler and Jones, 1990) now permits precise measurement of the effective polarizability of cells from several hertz to >50 MHz. In this work, we experimentally determine the real part of the effective polarizability of intact red blood cells (RBC) and pronase-treated red blood cells (PRBC) using dielectrophoresis (DEP) levitation. The data is used to estimate the temporal polarization response of cells to the field pulses used for electrofusion. The relative contribution of dipole–dipole interaction forces is then calculated and compared to experimental parameters affecting electrofusion. We will show that complementary relationships between membrane potential and the effective dipole–dipole interaction pressures exist across a broad range of frequencies and external media conductivities. The results presented here are important for resolution of fundamental physical force contributions in electrofusion, and may lead to possible technological improvements in cell hybridization.

GLOSSARY

ac	alternating current
BSS	balanced salt solution
DEP	dielectrophoresis
dc	direct current
PRBC	pronase treated red blood cells
RBC	red blood cells
rms	root-mean-square
S	Siemen
a, b, c	ellipsoid semiaxes
A	area of cell–cell contact region
$B_a(f)$	PRBC polarizability along the a semiaxis (frequency domain)
C_m	membrane capacitance per unit area
δ_{ieff}	effective internal membrane surface charge density
$E_0(t)$	amplitude of applied electric field
E_{0a}	electric field amplitude along the a semiaxis
$E_{a\,eff}$	effective electric field amplitude along the a semiaxis
$\epsilon = \epsilon - j\sigma/\omega$	complex relative permittivity (ϵ: dielectric constant, σ: conductivity)
ϵ_0	permittivity of free space
F_e	plate capacitor electrical force
L	erythrocyte shape factor
γ	erythrocyte geometric parameter
η	fusion medium viscosity
h_i	interbilayer separation
h_e	membrane dielectric (hydrophobic region) thickness
$Re[\mathbf{K_{eff}}]_a$	real component of the effective relative permittivity of a cell along the a semiaxis
$P_{a\,eff}(t)$	effective a semiaxis dipole moment
σ_e	specific conductance of the fusion medium
σ_i	cell internal specific conductance
σ_{3D}	dipole:dipole interaction-generated normal pressure
σ_{3T}	total electromechanical pressure normal to membrane surface
σ_{3v}	membrane potential-generated normal pressure
τ_m	membrane charging relaxation constant
τ_{pa}	polarization relaxation constant along a semiaxis
τ_{pc}	polarization relaxation constant along c semiaxis
V_m	induced membrane potential
V_{max}	maximum membrane potential (at cell poles)

THEORY

Pressure due to membrane potential

For dielectric response purposes, the human erythrocyte is sufficiently well modeled assuming an ellipsoidal shape (Kinosita and Tsong, 1977) and a perfectly insulating membrane. The membrane potential response of an ellipsoidal cell to arbitrary waveform electric pulses has been rigorously modeled (Jeltsch and Zimmermann, 1979). When such a cell having semimajor axes $a = b >$ semiminor axis c is exposed to a step function electric field parallel with a, E_{0a}, the membrane potential at the poles ($\pm a$) under stationary conditions may be described as:

$$V_{max} = faE_{0a}. \tag{1}$$

The shape factor f is:

$$f = 1 + 1/\gamma = 1/(1 - L_r), \tag{2}$$

where γ is the geometric parameter, and L_r is the elliptic integral along the r direction:

$$L_r = (abc/2) \int (s + r^2)^{-1} \cdot [(s + a^2)(s + b^2)(s + c^2)]^{-1/2}\, ds. \tag{4}$$

r is a, b, or c, and the integration is over the ellipsoid surface s.

When exposed to a step-function electric field, the membrane charges according to:

$$V_m(t) = V_{max}\,[1 - \exp(-1/\tau_m)], \tag{5}$$

with a membrane relaxation time τ_m:

$$\tau_m = aC_m\,(1/\sigma_i + 1/\sigma_e\gamma), \tag{6}$$

where C_m is the membrane capacitance per unit area, and σ_e and σ_i are the external and internal specific conductances, respectively. If, instead, the cell is exposed to a sinusoidal electric field (having angular frequency ω) parallel with a, the maximum amplitude of the superimposed membrane potential at the poles of the ellipsoid ($\pm a$) should be well approximated by

(Holzapfel et al., 1982):

$$V_{max} = faE_{0a}/\sqrt{1 + (\omega\tau_m)^2}. \quad (7)$$

For the human erythrocyte, we may assume average values for a and b of 3.9 μm (Canham et al., 1971), and c = 1.2 μm (Kinosita and Tsong, 1979). C_m has recently been measured to be relatively constant (0.70–0.75 μF/cm^2) across a broad frequency range (Takashima et al., 1988). σ_i has been measured to be 5.5 mS/cm (specific resistance = 1.8 × 10^2 ohm cm) (Pilwat and Zimmermann, 1985). Evaluation of Eq. 4 using the given ellipsoidal semiaxes gives a value for L_a of 0.16. The geometric parameter γ and shape factor then have respective values of 5.2 and 1.2, significantly different from the corresponding spherical values of 2.0 and 1.5. σ_e is the external conductivity and is thus an experimental parameter.

The normal electrical pressure, σ_{3v}, acting on the membrane due to the membrane potential is described as a symmetrical electrical pressure (Needham and Hochmuth, 1989):

$$\sigma_{3v} = 0.5\,\epsilon_e\epsilon_0\,(V_m/h_e)^2, \quad (8)$$

where h_e is the dielectric thickness of the membrane. The convention of σ_{3v} is used here to avoid confusion over the use of σ to denote conductivity.

For cells aligned along a pearl chain, the net electric field along the pearl chain axis should be modified due to the dipole field contribution. The effective electric field along the chain axis is considered to be the sum of the external electric field and the fields from two neighboring point dipoles, each separated by two times the semimajor axis, a:

$$E_{a\,eff} = E_{0a} + P_{a\,eff}/[2\pi\epsilon_0\epsilon_e\,(2a)^3], \quad (9)$$

where $P_{a\,eff}$ is the effective dipole moment of a cell as discussed below.

Pressure due to the induced effective dipole moment

The relative permittivities ϵ_i and ϵ_e of a dielectric particle and its suspending media, respectively, are complex quantities, expressed as (Pohl, 1978):

$$\epsilon = \epsilon - j\sigma/\omega, \quad (10)$$

where ε and 1/σ are the real and imaginary relative permittivity components. For an ellipsoidal particle exposed to an electric field E_{0a} parallel to the semiaxis a, steady-state effective dipole moment develops (Miller and Jones, 1987) as a function of the real component of the effective permittivity:

$$P_{a\,eff} = (4\pi abc/3) \cdot \epsilon_0\epsilon_e\,Re\,[(\epsilon_i - \epsilon_e)/[\epsilon_e + (\epsilon_i - \epsilon_e)L_a]]\,E_{0a}. \quad (11)$$

The real component of effective permittivity along the a-axis is defined as:

$$Re[\boldsymbol{K}_{eff}]_a = Re[(\epsilon_i - \epsilon_e)/[\epsilon_e + (\epsilon_i - \epsilon_e)L_a]]. \quad (12)$$

By introducing the effective a-axis polarizability B_a,

$$B_a = (4\pi abc/3)\,\epsilon_0\epsilon_e\,Re[\boldsymbol{K}_{eff}]_a, \quad (13)$$

Eq. 11 becomes

$$P_{a\,eff} = B_a E_{0a}. \quad (14)$$

The effective dipole moment at any given time t results from the superposition of the instantaneously and previously generated dipoles (Bottcher and Bordewijk, 1978; Holzapfel et al., 1982). Previously generated dipoles decay exponentially according to exp $(-t/\tau_{pa})$, where τ_{pa} is the relaxation time of the specific polarization mechanism along the a-axis. The time-dependent effective dipole moment is expressed as the convolution integral:

$$P_{a\,eff}(t) = (1/\tau_{pa}) \int B_a(t')\,E_{0a}(t')\,\exp[(t' - t)/\tau_{pa}]\,dt', \quad (15)$$

which is similar to the expression used by Holzapfel et al. (1982) except that B_a is not a constant but a complex quantity with both frequency and orientation dependency. Defining

$$H(t) = \exp(-t/\tau_{pa}), \quad (16)$$

and applying the convolution theorem (Jonscher, 1983), the convolution pair of

$$(1/\tau_{pa}) \int B_a(t')E_{0a}(t')H(t - t')dt' \leftrightarrow (1/\tau_{pa})B_a(f)E_{0a}(f)H(f), \quad (17)$$

may be used to relate the temporal response to the frequency-dependent polarizability $B_a(f)$. This transform pair allows the use of experimentally obtained values of $B_a(f)$ to calculate the temporal polarization response. The spectrum of $B_a(f)$ is determined by DEP levitation using the theory and apparatus described in Kaler and Jones (1990). For PRBC in this cone-plate electrode setup, the $Re[\boldsymbol{K}_{eff}] = 1.9/V_0^2$ where V_0 is the root-mean-square (rms) voltage across the electrode required to balance the DEP and gravitational forces.

For cells in a pearl chain, the effective dipole moment must be modified to take into account the image dipoles produced in neighboring cells and electrodes. The infinite expansion of image dipole effects has been evalu-

ated (Jones et al., 1986). The effect may be first-order approximated by multiplying the single particle moment by an enhancement factor n. For a three cell chain in contact with a metal electrode, the effective number of conducting particles becomes six, due to the development of three image dipoles within the electrode. Then, an enhancement factor of 10 should be applied to the single cell dipole moment of each cell in the chain (Jones et al., 1986).

When cells are drawn together by DEP forces, small portions of the apposed membrane elements are separated by $\ll 1$ μm. In these regions, the pressure across the apposed pair of membranes cannot be described by Eq. 8 alone. Instead, because the thickness of the closely contacting membrane pair is much less than the lateral dimension of the region, a plate capacitor model is proposed to account for additional pressures arising from effective dipole charge interactions. A simplified model of the close-contact region between DEP-aligned cells is shown in Fig. 1. The effective inner surface charge densities, $\delta_{i\,eff}$ and $-\delta_{i\,eff}$ which are concentrated on the inner membrane surface at the poles of each cell, are separated by a distance h. Here, h is equal to

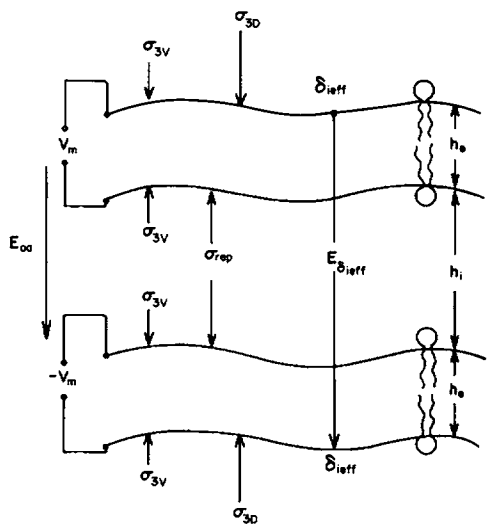

FIGURE 1 Simplified model of intra- and intermembranous forces within and between two polarized, closely positioned membranes. A potential gradient across each membrane, V_m, induces an electrical pressure σ_{3v} described by Eq. 8. The effective dipole moment of each cell arises from equal and opposite effective charge densities, $\delta_{i\,eff}$ and $-\delta_{i\,eff}$ at the opposite inner membrane surfaces. These surfaces interact with the attractive force described by Eq. 18. For a given region, this gives rise to the dipole–dipole interaction pressure σ_{3D} acting on the inner membrane surfaces. If this pressure, coupled with other attractive contributions (i.e., Van der Waals pressure) is greater than the repulsion at the separation h_i, the intermembrane separation is reduced.

$(2h_e + h_i)$, where h_e is the dielectric thickness of the membrane and h_i is the interbilayer thickness, inclusive of the phospholipid headgroup regions. The value of h_e used here is 3.3 nm, corresponding to the value used by Needham and Hochmuth (1989) for liposomes prepared from erythrocyte lipid extracts.

The electrical force between the two effective surface charge densities is described as (Wangsness, 1979):

$$F_e = -Q^2/2\epsilon_0\epsilon_e' A, \tag{18}$$

where Q is the total effective charge on each surface of the area A. To a first order approximation,

$$Q = \delta_{i\,eff} A = P_{a\,eff}/2a. \tag{19}$$

Based on previous phase microscopic observations, a typical circular contact area has a radius of ~ 1 μm. ϵ_e' represents the weighted average of ϵ_e and the dielectric constant of the membrane hydrophobic region. If most of the interbilayer medium is extruded, the separation between the two effective charge distributions approaches $2h_e$. The real interbilayer permittivity component, ϵ_e' will then approach the value of the membrane hydrophobic region, taken here to be 2.2 (see the next section). Thus, the dipole–dipole interaction-generated normal pressure acting on the apposed contact area:

$$\sigma_{3D} = F_e/A = \delta_{i\,eff}^2/2\epsilon_0\epsilon_e' = P_{a\,eff}^2/(8\epsilon_0\epsilon_e' a^2 A^2) \tag{20}$$

Therefore if $P_{a\,eff}(t)$ is known, the pressure σ_{3v} and σ_{3D} may be derived from the first principle.

Intra- and interbilayer events during pulse application

Direct bilayer contact between erythrocyte membranes is opposed by the electrostatic, hydration (Parsegian et al., 1984), steric, osmotic (Bell et al., 1984), and other forces. When the attractive force due to dipole–dipole interaction exceeds the repulsion at a given separation, the water is extruded from the region, or forced through the membrane. Dimitrov (1983) has shown theoretically that the thinning rate of a cylindrical film of thickness h (consisting of bulk water) for negligible inertial forces is:

$$-(dh_i/dt) = Fh/3\pi\eta R^2, \tag{21}$$

where F is the net force on the film, η is the medium viscosity, and R is the cylindrical area radius. This is a reasonable reflection of the situation during the 5–50 μs of pulse time, because the viscoelastic relaxation constant for RBC surface deformations is on the order of 100 ms (Hochmuth et al., 1979; Engelhardt and Sack-

mann, 1988) implying solid-like behavior of the membrane during the pulse.

Because the reduction of the interbilayer distance is continually opposed by repulsive and hydrodynamic forces (Dimitrov, 1983), the membrane will experience a pressure equal that caused by the attractive dipole–dipole interactions, in addition to that caused by the membrane potential. The total normal pressure σ_{3T} acting on each of the apposed membrane areas during pulse application is then considered as the linear sum of σ_{3v} and σ_{3D},

$$\sigma_{3T} = \sigma_{3v} + \sigma_{3D}. \quad (22)$$

Hence, the membrane may be forced to rupture by either excessive membrane potential, excessive dipole–dipole interaction pressures, or a combination of both.

When Eq. 18 is evaluated for a 3 *kV*/cm field amplitude, $\epsilon_e = 80$, and is divided by the contact area A, a force per unit area in the close-contact region of ~ 1–2×10^5 dyn/cm^2 is obtained. This value corresponds to the repulsion pressure observed between lipid bilayers at separations of 2–3 nm, just greater than the hydration thickness (Parsegian et al., 1984). The initial rate of interbilayer reduction, as estimated by Eq. 21, for a net force of $\sim$ (10^5 dyn/cm^2) $\times$ (3.14×10^{-8}cm^2) and a separation of 15 nm (Stenger and Hui, 1986), is on the order of 1–2 cm/s. A reduction of h_i by 10–13 nm would then be possible in the time range of 1 μs. This means that even the transient dipole moment generated at the leading edge of a 3 kV/cm rectangular pulse would produce a sufficient dipole–dipole interaction pressure to extrude much of the bulk water from the interbilayer region. This calculation corresponds well to the observation (Stenger and Hui, 1986) that the interbilayer separation was reduced to 2–3 nm after rectangular pulse application. Because the pressure can be much higher in the case of sinusoidal pulses, it is appropriate to consider that the permittivity of the region separating the effective charge distributions approaches that of the membrane hydrophobic region during pulse application.

MATERIALS AND METHODS

Human erythrocytes were separated from freshly drawn whole blood, washed twice in balanced salt solution (BSS) at pH 7.4. For pronase treatment, a 1:10 (vol:vol) dilution of pellet was incubated at 37°C for 30 min in BSS containing 3 mg/ml pronase E (Sigma Chemical Co., St. Louis, MO). Degradation of membrane proteins by the pronase treatment was analyzed in previous work (Stenger and Hui, 1986).

A detailed description of DEP levitation principles applied to the study of the polarization phenomena of biological cells is available elsewhere (Kaler and Jones, 1990). To provide a low conductivity suspension medium of minimal viscosity, 0.28 M inositol (Sigma Chemical Co.) was used. The specific conductivity of the inositol in distilled, deionized water was ~15 μS/cm at 22°C. 1.5 μl of cell/BSS pellet was added to 1.0 ml of inositol media. This caused less than a 1.0 μS/cm conductivity increase which was considered insignificant. Additional media having conductivities of 150 and 650 μS/cm were prepared by addition of up to several millimolar concentrations of KCl to the base inositol solution.

The temporal polarization responses of PRBC to applied rectangular and sinusoidal electric field pulses were calculated using a C language (Microsoft Corp, Redmond, WA) simulation program and performed on a PS/2 computer (IBM Instruments, Inc., Danbury, CT).

Electrofusion was conducted in a fusion chamber designed for an approximately uniform electric field. Fusion chambers were constructed using parallel arrangements of rectangular platinized stainless steel electrodes arranged at separations of 100 μm. The electronic equipment used for generating the ac field and rectangular pulses has been previously described (Stenger and Hui, 1988). As a variation in some experiments, gated bursts of high-voltage ac were used as a substitute for rectangular pulses. The term "pulse" is used in the generic sense to describe both dc pulses and gated bursts of purely sinusoidal voltage.

The cells were aligned by DEP using a 2.5-MHz ac field. This frequency was chosen to ensure DEP polarization which was independent of the particular external conductivity chosen. A marginal ac field (peak) amplitude of 300 V/cm was chosen to favor shorter chain formation (two to four cells), and to prevent significant temperature increases and cell deformation. The temperature increase after 30 s of ac field application was measured for each media by positioning a thermocouple in the electrode gap. The increase was <3°C for all media.

All fusion experiments were visualized by phase microscopy (Olympus model BH-2; Olympus Corporation of America, New Hyde Park, NY), and recorded using a video recorder (model AG-6050; Panasonic Industrial Co., Secaucus, NJ). A single electric pulse was used for each experiment. Video recordings of the individual trials were reviewed. The fusion threshold was set such that at least 75% of all the 3 cell pearl chains completely fused following pulse application. Error bars indicate the amplitude variation within a pulse and estimated error due to field strength uncertainty.

RESULTS AND DISCUSSION

DEP levitation

Pronase treatment facilitates erythrocyte electrofusion (Stenger and Hui, 1986). The DEP levitation spectra from 20 Hz to 50 MHz for pronase treated erythrocytes in three media with conductivities in the range of 15–650 μS/cm are shown in Fig. 2. Cells aligned with their disc radius parallel to the external field at frequencies <10 MHz in all external media used. The magnitude of the voltage squared (V^2 rms) across the conical electrode required to balance the DEP and gravitational forces is plotted as a function of frequency. The $Re\{K_{eff}\}_a$ is inversely related to V_0^2.

At frequencies $>10^4$ Hz, the PRBC behaved in a manner consistent with that predicted by Maxwell-Wagner interfacial polarization theory. The frequency range over which the cells exhibited positive DEP was strongly dependent on the conductivity of the suspending media. As the conductivity was increased from 15 to 650 μS/cm, the low frequency limit for positive DEP

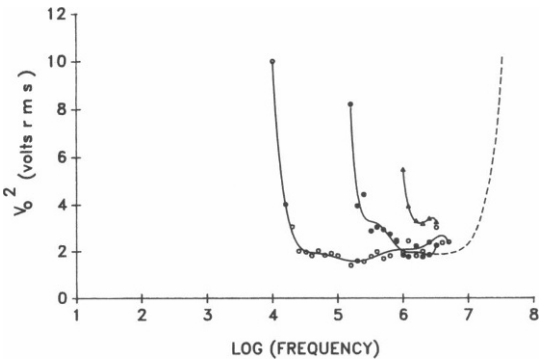

FIGURE 2 DEP levitation spectra from 20 Hz to 50 MHz for pronase-treated erythrocytes in media of different conductivities. Solid lines represent direct experimental curves, the dashed line represents the asymptotic extrapolation of the increasing values of V_0^2 as the reorientation frequency is approached. Open circles = 15 μS/cm, closed circles = 150 μS/cm, open triangles = 650 μS/cm.

increased from ~10^4 to 10^6 Hz. Within the positive DEP frequency ranges, cells exhibited approximately the same level of polarizability regardless of the media conductivity.

In the 10–20 MHz range, the PRBC major axis reoriented perpendicular to the applied field. The levitation spectra showed small increases in the values of V_0^2. The perpendicular orientation was maintained throughout the 20–50 MHz frequency range. The reorientation frequency corresponds to the reciprocal of τ_{pa}, the internal ion polarization relaxation time constant along the *a* axis. After reorientation, the V_0^2 values for these media nearly returned to the baseline value in the 30 MHz range followed by asymptotically increasing values at frequencies of 30–50 MHz. The upper frequency limit for positive DEP is approached as the frequency becomes equal or $> 1/\tau_{pc}$, where τ_{pc} is the relaxation time of the polarization mechanism along the *c*-axis. The increasing values of V_0^2 are extrapolated asymptotically with frequency (Fig. 2, *dashed lines*) to simulate simple Debye-type relaxation of cells restricted to the parallel orientation (Hui and Stenger, 1991). Solid lines represent curves of actual experimental data.

Within the DEP range, the $Re\{\boldsymbol{K}_{eff}\}_a$ for the cells may be derived from the observed values of V_0^2 (Kaler and Jones, 1990). For both intact RBC and PRBC, the minimum value of V_0^2 is ~2.0 V, corresponding to a $Re\{\boldsymbol{K}_{eff}\}_a$ of ~0.95. This implies that within a given frequency range, PRBC behave as nearly ideal conductors, which exhibit a $Re\{\boldsymbol{K}_{eff}\}_a = 1$. As will be shown later, this has very significant consequences for the magnitude of dipole moments which develop in chains of DEP-aligned cells.

Calculation of temporal polarization responses

Calculation of pulse-induced dipole moments of PRBC were performed as a function of the electric pulse amplitude, waveform, and external conductivity. The frequency domain polarizability, $B_a(f)$, as obtained from the levitation data, was an approximately constant value of 4×10^{-26} (coulomb m^2)/V in the frequency ranges where positive DEP levitation occurred. The low frequency limits of 1.0×10^4 Hz, 2.0×10^5 Hz, and 1.0×10^6 Hz were defined for PRBC suspended in the 15, 150, and 650 μS/cm media, respectively. The upper frequency limit for positive DEP, obtained by extrapolation, was set at 3.0×10^7 Hz. The reciprocal of this value, 3.33×10^{-8} seconds for all three media, was assigned as the polarization relaxation time, τ_{pa}.

The temporal polarization $P_{a\,eff}(t)$ is then calculated using Eq. 15–17, for representative fusion-inducing pulses duration, frequency (if sinusoidal) and fusion media conductivity. In several cases, the pulses have amplitudes which are found to produce supercritical membrane potentials leading to membrane breakdown. In such cases it is assumed that a linear dielectric response will proceed until at least the time point when membrane breakdown occurs. It is noteworthy that even after dielectric breakdown, much of the prebreakdown charge distributions about the membrane remain, as indicated by pulsed laser fluorescence (Kinosita et al., 1988).

Fig. 3 shows two representative, calculated effective single cell dipole responses, $P_{a\,eff}(t)$ to a 10 μs, 4.0 kV/cm rectangular pulse. A bandpass-filtered response occurs because $B_a(f)$ is nonzero for only a finite range of frequencies at each conductivity. Fig. 3 *a*, illustrating the PRBC $P_{a\,eff}(t)$ response in 650 μS/cm media, shows that high frequency components at the leading edge of the pulse cause the moment to increase with the rising field amplitude (the pulse rise and fall time is 170 ns). For most of the pulse length the response is dominated by the lower cutoff frequency (10^6 Hz) of $B(f)$. Because the fundamental frequency of the pulse (10^5 Hz corresponding to 10 μs) is outside the $B(f)$ bandwidth, the contribution to $\int P_{a\,eff}(t)\,dt$ is zero throughout the pulse length. At the end of the 10 μs pulse, out-of-phase high frequency components turn the moment negative on the trailing edge. The moment decays exponentially back to zero with the time constant τ_{pa}. Similar results were obtained when the same calculation is performed for the 15 and 150 μS/cm media (not shown).

Fig. 3 *b* shows the calculated $P_{a\,eff}(t)$ responses to a 35 μs, 100 kHz sinusoidal pulse. Because the applied frequency is within the 15 μS/cm polarizability bandwidth, the response is large and is approximately sinusoidal. This frequency dependence is held for all sinuso-

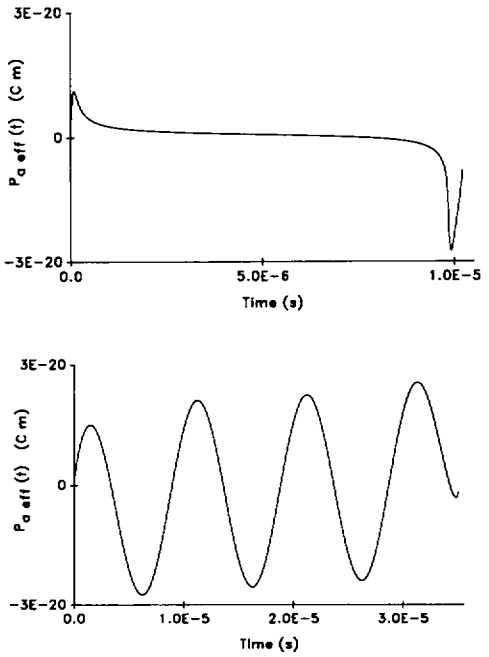

FIGURE 3 Calculated single cell effective dipole response (*a*) to a single 4.0 kV/cm, 10 μs rectangular pulse for PRBC suspended in 650 μS/cm media, and response (*b*) to a single 3.0 kV/cm, 35 μs duration, 100 kHz sinusoidal pulse for PRBC suspended in 15 μS/cm media.

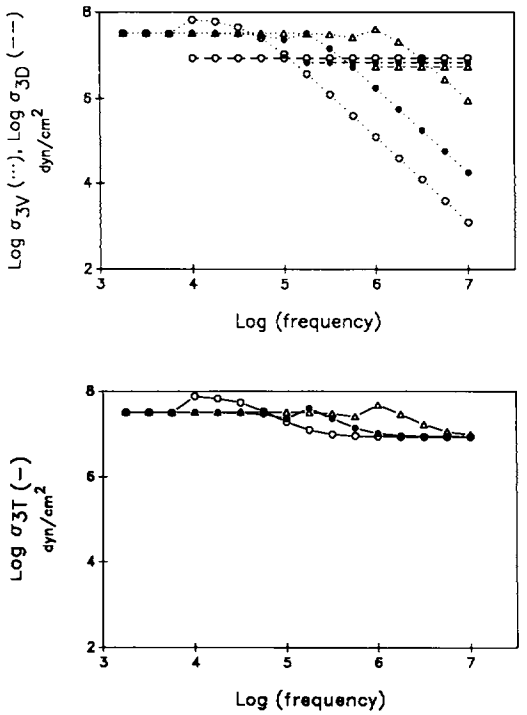

FIGURE 4 Calculated (*a*) individual contributions of the maximum normal pressure acting across the membrane due to membrane potential σ_{3v} (*dotted lines*), and dipole–dipole interactions, σ_{3D} (*dashed lines*) and (*b*) total pressure σ_{3T} in response to a 4.0 kV/cm (*peak*) sinusoidal pulse as a function of frequency. Open circles = 15 μS/cm, closed circles = 150 μS/cm, open triangles = 650 μS/cm.

idal pulses in the range of 100 kHz–2.5 MHz. For PRBC in both 150 and 650 μS/cm media (not shown), the response is small for 100 kHz pulse because the pulse frequency is outside of the polarizability bandwidths for these media.

Calculation of membrane potential

The maximum membrane potential at the poles of the cells for different applied field strengths and experimental conditions were calculated. For rectangular pulses, Eq. 1 predicts a membrane potential of 1.0 V when a field of 2.2 kV/cm is applied along the semimajor axis of the cell. Because field amplitudes of 2.0–2.5 kV/cm are the observed threshold values for the increased conductance of erythrocyte membranes in a number of dielectric breakdown experiments (Zimmermann et al., 1974; Kinosita and Tsong, 1979) a "critical" V_m of 1.0 V at the poles of the cell will be assumed for dielectric breakdown at 20°C. The membrane potential developed during a 10–50 μs pulse, of amplitude 2.5–9 kV/cm were calculated for both rectangular and sinusoidal pulses, using Eq. 7. Eq. 6 predicts membrane relaxation times τ_m of 3.8, 1.0, and 0.14 μs for the 15, 150, and 650 μS/cm media, respectively. Thus, according to Eq. 5, for pulse widths of 10 μs or longer, the maximum membrane potential was not limited by charging time in any of the three media.

The calculated threshold amplitudes of rectangular pulses reaches supercritical values of V_m, even at $E_0 = 3$ kV/cm, independent of the external conductivity. For sinusoidal pulses, Eq. 7 depicts that the value of V_m at a fixed frequency increases with increasing external medium conductivity because of the $\omega\tau_m$ dependency. For $E_0 = 3$ kV/cm, the calculated V_m values for 100 kHz pulses exceed the critical 1.0 V only in 150 and 650 μS/cm media. In the case of 2.5 MHz pulses, it requires 5.5 kV/cm pulse field strength in 650 μS/cm media to reach the critical V_m values of 1.0 V.

Lower frequencies and higher external conductivities favor development of supercritical fields as predicted by Eq. 7. For cells in a three cell chain, the V_m value is enhanced by Eq. 9. For rectangular pulses in these three media, the effective dipole existence is limited to the leading and trailing edges of the pulse. Thus, for most of the pulse duration, the dipole field contribution is negligible. However, for sinusoidal pulses having frequencies within the polarizability bandwidth of the cell at a

given external conductivity, there is a minor dipole field contribution for the entire pulse duration.

Calculation of σ_{3T}, σ_{3v}, and σ_{3D}

The rms dipole–dipole interaction pressure σ_{3D} was calculated for an effective charge of $P_{a\,eff}(t)/2a$ distributed uniformly across 1 μm radius, circular contact areas at a separation of <2 nm, using Eq. 20. A value of 2.2 was used for ϵ_e' corresponding to that reported for erythrocyte lipids (Needham and Hochmuth, 1989).

Fig. 4 *a* serves to illustrate the calculated magnitudes of the individual σ_{3v} and σ_{3D} contributions for the three media used in response to a 4.0 kV/cm sinusoidal pulse as a function of frequency according to Eqs. 8 and 20, respectively. The calculated σ_{3v} values (Fig. 4, *dotted lines*) decrease significantly for each of the three media used when the frequency becomes $>1/\tau_m$. However, because the polarizability is considered to be constant for finite ranges of frequencies, the calculated σ_{3D} values (Fig. 4, *dashed lines*) are constant from the low frequency cutoff points through 10^7 Hz, and zero outside the polarizability bandwidths.

Fig. 4 *b* shows the sum of the individual calculated σ_{3v} and σ_{3D} contributions for the same conditions shown in Fig. 4 *a*. Despite large differences of the individual contributions across the frequency range shown, the calculated σ_{3T} decreases only by about a factor of ten for the different media. More significantly, when the two rms (peak for rectangular) contributions are summed and multiplied by the pulse duration Δt for experimentally obtained threshold pulses, the product $\sigma_{3T}\Delta t$ falls within a factor of two for nearly all experimental threshold pulses, ranging from 1.75–4.03 $\times$ 10^2 (dyn s)/cm.

Measurement of fusion threshold field amplitudes

Because the magnitude of image dipoles which develop in chains of ideal conductors depends on the number of particles, fusion was monitored only for chains with a fixed number (three) of cells. The same 15, 150, and 650 μS/cm conductivity 0.28 M inositol media used for DEP levitation were used for fusion. Fusion was induced by application of a single electric pulse which was either rectangular (dc) or a burst of sinusoidal voltage. The frequency of the sinusoidal electric field burst was varied from 100 kHz to 2.5 MHz. A positive electrofusion sequence is illustrated in Fig. 5.

Fig. 6 *a* shows the threshold fusion field amplitudes for rectangular pulses having durations of 10–50 μs for different external conductivities. The fusion threshold field amplitudes remained essentially constant for pulses

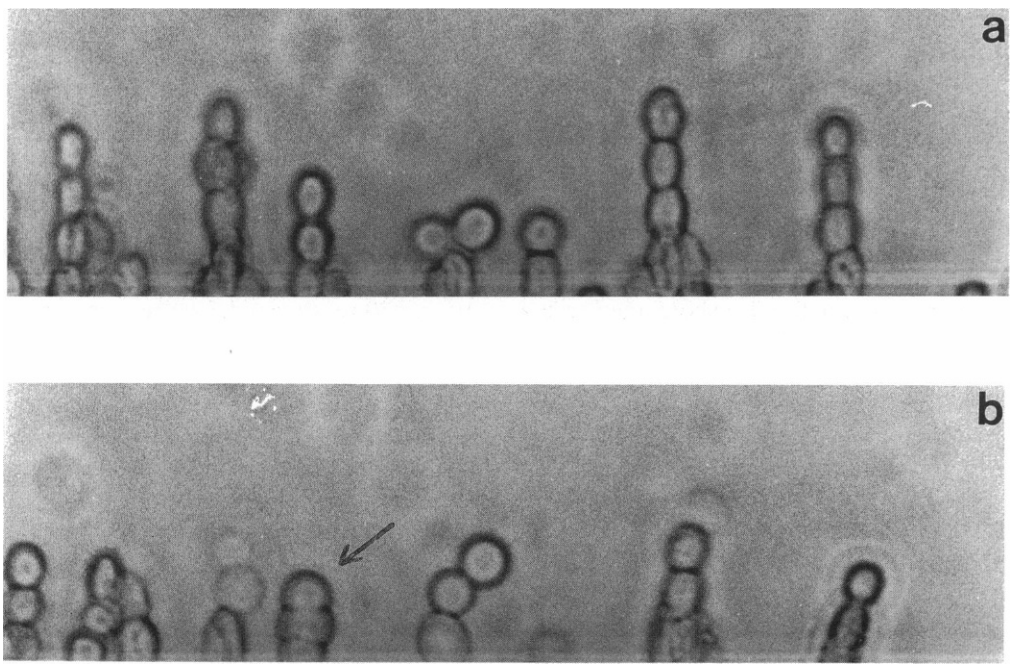

FIGURE 5 Positive electrofusion trial. Cells were DEP aligned in a 300 V/cm, 2.5 MHz ac field. Fusion was induced by application of a single 4.0 kV/cm, 10 μs rectangular pulse. (*a*) DEP alignment and selection of three cell PRBC chains for observation (*b*) arrow points to a three cell fusion product.

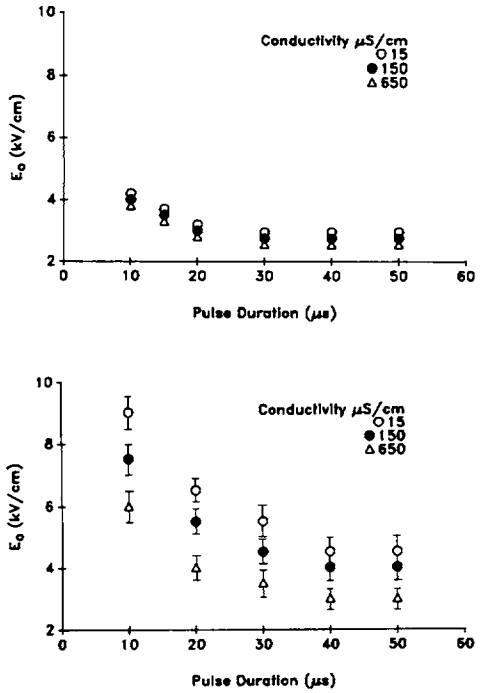

FIGURE 6 Threshold electric field amplitudes necessary for fusion as a function of duration for various external conductivities for (*a*) rectangular (dc) pulses and (*b*) 750 kHz sinusoidal bursts.

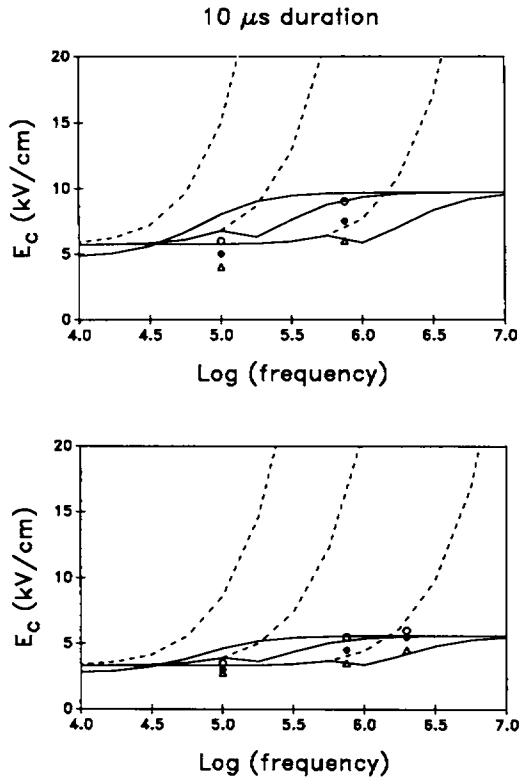

FIGURE 7 Theoretical curves calculated by accounting for dipole interaction pressures (*solid lines*), without accounting for dipole interaction pressures (*dashed lines*) and experimentally obtained (data points) threshold field amplitudes for (*a*) 10 μs, and (*b*) 30 μs sinusoidal pulses as a function of frequency. The top, middle, and bottom solid line curves and the left, middle, and right dashed line curves correspond in each case to 15, 150, and 650 μS/cm media, respectively. Data points: open circles = 15 μS/cm, closed circles = 150 μS/cm, and open triangles = 650 μS/cm.

at durations >30 μs. At low conductivity (15 μS/cm), the PRBC had slightly higher thresholds than at higher conductivities. For pulses of durations <20 μs, thresholds increased for decreasing duration in all three media.

Fig. 6 *b* illustrates the experimentally observed field thresholds for 750 kHz sinusoidal pulses of variable duration. The threshold amplitudes are slightly higher than those for rectangular pulses of the same duration, as expected from Fig. 4. Again, the threshold amplitudes became duration dependent, at shorter pulse durations, increasing in all cases for pulse durations of <30 μs. Similar responses were also observed for 100 kHz and 2.5 MHz pulses (not shown).

Comparison of experimental and theoretical threshold field amplitudes

The narrow range of calculated $\sigma_{3T}\Delta t$ values predicted that threshold field amplitudes for most pulses of ~ 10–30 μs duration should be of the same order of magnitude. This is consistent with the assumption that the PRBC behaves as a linear dielectric material with an empirical threshold $\sigma_{3T}\Delta t$ value of 3.25×10^2 (dyn s)/cm^2 for membrane fusion, representing the average value obtained for 15 μS/cm media with 2.5 MHz pulses (when the membrane potential contribution is minimized).

The experimentally obtained threshold amplitudes for 10 and 30 μs sinusoidal pulses are superimposed on the theoretical solid lines in Fig. 7 *a* and *b*, respectively, as a function of pulse frequency. The dashed lines in Fig. 7, *a* and *b*, represent the theoretical critical fields for the same value of $\sigma_{3T}\Delta t$ if dipole interaction pressure σ_{3D} is not accounted for. Although the low frequency values are quite similar, the theoretical threshold field amplitude increases exponentially at higher frequencies to values several orders of magnitude higher than that observed experimentally.

CONCLUSION

In this study, we have defined the major factors contributing to the electrofusion of adjacent cells suspended in

low conductivity (15–650 μS/cm) media. The fusion threshold field can be roughly predicted over the range of frequencies and external conductivities used only if the transverse membrane pressures due to membrane potential and induced dipole interaction are taken into consideration. The contribution of dipole-induced pressure ensures that σ_{3T} remains approximately constant over the wide range of frequency and external conductivity. At low frequencies and in high external conductivity media, the membrane potential alone appears sufficient to account for membrane breakdown. However, at high frequency and in low conductivity media, the induced dipole contribution appears to become dominant. The contribution of the dipole field also explains the higher field strength needed to permeate isolated cells than to fuse cells in chains. The calculated values for σ_{3T} were within the range of $1–3 \times 10^7$ dyn/cm^2. This range is consistent with that implied by Eq. 9 from the experimental work of Needham and Hochmuth (1989), although they did not measure the time dependence of the events.

It should be emphasized that the theoretical model and data presented here pertain only to the specific set of experimental conditions used (i.e., PRBC in very low conductivity media). It is likely that other electrofusion protocols using high conductivity media and pulses with a significant dc frequency component (Sowers, 1984; Chang, 1989) will involve much less contribution from dipole–dipole interaction. However, it is possible also that the low frequency ($< 10^3$ Hz), surface ion polarization exhibited by intact RBC (Hui and Stenger, 1991) could play a significant role in those situations.

We would like to thank Dr. Robert Spangler (Biophysical Sciences, State University of New York at Buffalo) and Dr. Thomas Jones (Electrical Engineering, University of Rochester) for their guidance in the theoretical aspects of this work, and Alan K. C. Tai (Electric Engineering, University of Calgary) for experimental assistance in dielectrophoresis (DEP) levitation.

This work was supported by National Institutes of Health grant number GM30969 awarded to S. W. Hui and National Research Council of Canada grant number 4970 awarded to K. Kaler. The computer control software was written by Ron Platt. Data acquisition hardware was donated by Medtronics Canada, LTD., DEP levitation (Montreal).

Received for publication 6 December 1989 and in final form 29 January 1991.

REFERENCES

Bell, G. I., M. Dembo, and P. Bongrand. 1984. Cell adhersion in competition between nonspecific repulsion and specific bonding. *Biophys. J.* 45:1051–1064.

Bottcher, C. J. F. and P. Bordewijk. 1978. Theory of Electric Polarization. Vol. II: Dielectrics in Time-Dependent Fields. Elsevier Science Publishers B. V., Amsterdam.

Canham, P. B., A. W. L. Jay, and E. Tilsworth. 1971. The rate of sedimentation of individual human erythrocytes. *J. Cell. Physiol.* 78:319–332.

Chang, D. C. 1989. Cell poration and fusion using an oscillating electric field. *Biophys. J.* 56:641–652.

Dimitrov, D. S. 1983. Dynamic interactions between approaching surfaces of biological interest. *In* Progress in Surface Science. S.G. Davison, editor. Pergamon Press, New York. 14:295–424.

Engelhardt, H., and E. Sackmann. 1988. The measurement of shear elastic moduli and viscosities of erythrocyte plasma membranes by transient deformation in high frequency electric fields. *Biophys. J.* 54:495–508.

Hochmuth, R. M., P. R. Worthy, and E. Evans. 1979. Red cell extensional recovery and the determination of membrane viscosity. *Biophys. J.* 26:101–114.

Holzapfel, C., J. Vienken, and U. Zimmermann. 1982. Rotation of cells in an alternating electric field: theory and experimental proof. *J. Membr. Biol.* 67:13–26.

Hui, S. W., and D. A. Stenger. 1991. Effects of intercellular forces on electrofusion. *In* Handbook of Electrofusion and Electroporation. D. Chang, B. Chassy, J. Saunders, and A. Sowers, editors. Academic Press Inc., San Diego. In Press.

Jeltsch, E., and U. Zimmermann. 1979. Particles in a homogeneous electrical field: a model for the electrical breakdown of living cells in a coulter counter. *Bioelectrochem. Bioenerg.* 6:349–384.

Jones, T. B. Multipole corrections to dielectrophoretic force. 1985. *IEEE (Inst. Electr. Electron. Eng.) Trans. Indust. Appl.* IA-21:930–934.

Jones, T. B., and J. P. Kraybill. 1986. Active feedback-controlled dielectrophoretic levitation. *J. Appl. Phys.* 60:1247–1252.

Jones, T. B., R. D. Miller, K. S. Robinson, and W. Y. Fowlkes. 1986. Multipolar interactions of dielectric spheres. *J. Electrostatics.* 22:231–244.

Jonscher, A. K. 1983. Dielectric Relaxation in Solids. Chelsea Dielectrics Press, London. 36–53.

Kaler, K. V. I. S., and T. B. Jones. 1990. Dielectrophoretic levitation of single cells determined by feedback-controlled levitation. *Biophys. J.* 57:173–182.

Kaler, K. V. I. S., and A. K.-C. Tai. 1988. Dynamic (active-feedback controlled) dielectrophoretic levitation of canola protoplasts. *IEEE Engineering in Medicine and Biology conference.* New Orleans, LA. 267–268.

Kinosita, K., and T. Y. Tsong. 1977. Voltage-induced pore formation and hemolysis of human erythrocytes. *Biochim. Biophys. Acta.* 471:227–242.

Kinosita, K., and T. Y. Tsong. 1979. Voltage-induced conductance in human erythrocyte membranes. *Biochim. Biophys. Acta.* 554:479–497.

Kinosita, K., I. Ashikawa, N. Saita, H. Yoshimura, H. Itoh, K. Nagayama, and A. Ikegami. 1988. Electroporation of cell membrane visualized under a pulsed-laser fluorescence microscope. *Biophys. J.* 53:1015–1019.

Miller, R. D., and T. B. Jones. 1987. Frequency-dependent orientation of ellipsoidal particles in a. c. electric fields. *IEEE Ninth Annual Conference of the Engineering in Medicine and Biology Society. Boston, MA.* 710–711.

Needham, D., and R. M. Hochmuth. 1989. Electro-mechanical permeabilization of lipid vesicles: role of membrane tension and compressibility. *Biophys. J.* 55:1001–1009

Parsegian, V. A., R. P. Rand, and D. Gingell. 1984. Lessons for the study of membrane fusion from membrane interactions in phospholipid systems. *In* Cell Fusion. Ciba Foundation Symposium. Pitman Books Ltd. London. 1984. 9–27.

Pilwat, G., and U. Zimmermann. 1985. Determination of intracellular conductivity from electrical breakdown measurements. *Biochim. Biophys. Acta.* 820:304–314.

Pohl, H. A. 1978. Dielectrophoresis. Cambridge University Press, London.

Sauer, F. A., and R. W. Schlogl. 1985. Torques exerted on cylinders and spheres by external electromagnetic fields. A contribution to the theory of induced cell rotation. *In* Interactions Between Electromagnetic Fields and Cells. A. Chiabrera, C. Nicolini, and H. P. Schwan, editors. Plenum Publishing Corp., New York. 203–251.

Sowers, A. E. 1984. Characterization of electric field-induced fusion in erythrocyte ghost membranes. *J. Cell Biol.* 99:1989–1996.

Stenger, D. A., and S. W. Hui. 1986. The kinetics of ultrastructural changes during electrically-induced fusion of human erythrocytes. *J. Membr. Biol.* 93:43–53.

Stenger, D. A., and S. W. Hui. 1988. Human erythrocyte electrofusion kinetics monitored by aqueous contents mixing. *Biophys. J.* 53:833–838.

Takashima, S., K. Asami, and Y. Takahashi. 1988. Frequency domain studies of impedance characteristics of biological cells using micropipet technique. I. Erythrocyte. *Biophys. J.* 54:995–1000.

Wangsness, R. K. Electromagnetic Fields. 1979. John Wiley & Sons, New York.

Zimmermann, U. 1986. Electrical breakdown, electropermeabilization and electrofusion. *Rev. Physiol. Biochem. Pharmacol.* 105:176–256.

Zimmermann, U., G. Pilwat, and F. Riemann. 1974. Dielectric breakdown of cell membranes. *Biophys. J.* 14:881–899.